JOURNAL OF MATERIALS SCIENCE 33 (1998) 5255–5258

Microstructural analysis of the calcium aluminosilicate (CAS) glass-ceramic matrix in SiC_f/CAS composites deformed at a high temperature

YUN-MO SUNG*, SEUNG-JOON HWANG
Department of Materials Science and Engineering, Daejin University, Pochun-koon, Kyunggi-do 487-711, South Korea
E-mail: ymsung@road.daejin.ac.kr

The calcium aluminosilicate (CAS: anorthite) glass-ceramic matrix materials in the SiC_f/CAS composites deformed in compression at a high temperature were analyzed for microstructures. The matrix region right above the top of the SiC fiber ($\theta \sim 0^\circ$) showed high density of dislocations as well as twins. On the other hand, the matrix region remote from the top of the SiC fiber ($\theta \sim 90^\circ$) showed only a twinned structure. This experimental result was compared with the Meyer *et al.*'s mechanical modeling indicating that the interfacial traction of the matrix region right on the top of the fiber is significantly high compared to the remote stress and thus it rate limits the creep deformation of the composite.

1. Introduction

There has been considerable interest in silicon carbide fiber reinforced ceramic or glass-ceramic matrix composite materials mainly due to their high fracture toughness [1–5]. A previous microstructural analysis of the composite material indicates the existence of a distinct layer of partially graphitic carbon approximately 80 nm in thickness, forming directly on the SiC fiber from oxidation of SiC [1–5]. This graphite layer between the fiber and matrix enhances the fracture toughness of the composite.

High temperature mechanical properties of these composites have been studied as well since they are one of the promising structural refractory materials [6–9]. All of the composites studied previously showed improved creep properties compared to the unreinforced matrix materials. Meyer *et al.* [9] established a model to predict the high temperature mechanical response of SiC fiber reinforced calcium aluminosilicate (CAS) composites. Fig. 1 shows a compression specimen (a) and a unit-cell micromodel (b). Here, ϕ is the angle between applied load (σ_{yy}) axis (y) and the SiC fiber axis (x), and θ that, between the applied load (y) and interface normal traction (n). As shown in Fig. 2, the Meyer *et al.*'s model predicted that the interface tractions along the top of the fiber ($\theta \sim 0^\circ$) are substantially higher than the applied remote stress (Note that $t_n/\sigma_{yy} = 1.7$ at the top of the fiber: $\theta \sim 0^\circ$), whereas the tractions along $\theta > 40^\circ$ are zero for $\phi = 60^\circ$ sample. Thus, the region right above the fiber would be stressed significantly above the far field applied stress level. Furthermore, the sample with $\phi = 90^\circ$ showed zero traction at $\theta > 37^\circ$. Accordingly, for a composite sample ($\phi = 90^\circ$) the matrix of $\theta = 0^\circ$ would be expected to show high density of dislocations and that of $\theta > 37^\circ$ low density. Several previous investigators have found a large number of twins and dislocation glide for the deformation of the naturally occurring anorthite, plagioclase feldspar [10, 11].

The focus of present study is on the investigation of the microstructure of the calcium aluminosilicate matrix in the SiC_f/CAS composites deformed at a high temperature. This experimental result was compared with the prediction of the Meyer *et al.*'s model.

2. Experimental

The composite materials used for this study were manufactured by Corning Inc., consisting of unidirectional Nicalon® silicon carbide fiber (30 vol %) and calcium aluminosilicate (CAS) glass-ceramic matrix. The calcium aluminosilicate composition used as the matrix lies on the corundum (Al_2O_3)–anorthite ($CaAl_2Si_2O_8$) binary join (~ 7 wt % of Al_2O_3) of the CaO-Al_2O_3-SiO_2 ternary system. The CAS matrix material shows grain size of about 1–3 μm, whereas the SiC fibers show extremely fine grain size of about 1.5 nm. The diameter of the SiC fiber was approximately 15 μm. The composites deformed by compressive creep tests ($\sigma_{yy} =$ 35 MPa) at 1290 °C and in an argon gas atmosphere, were used for present microstructural analysis study.

* Author to whom all correspondence should be addressed.

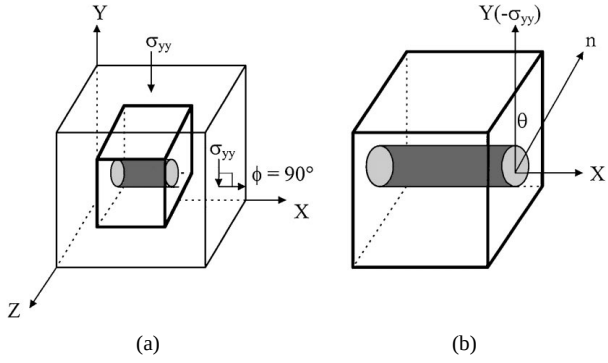

Figure 1 Schematics of (a) compression specimen with compressive loading (σ_{yy}), (b) unit-cell microscale model. The ϕ corresponds to the angle between the compressive axis (y) and fiber direction (x); the θ that between the compressive axis (y) and the normal traction (n) [6].

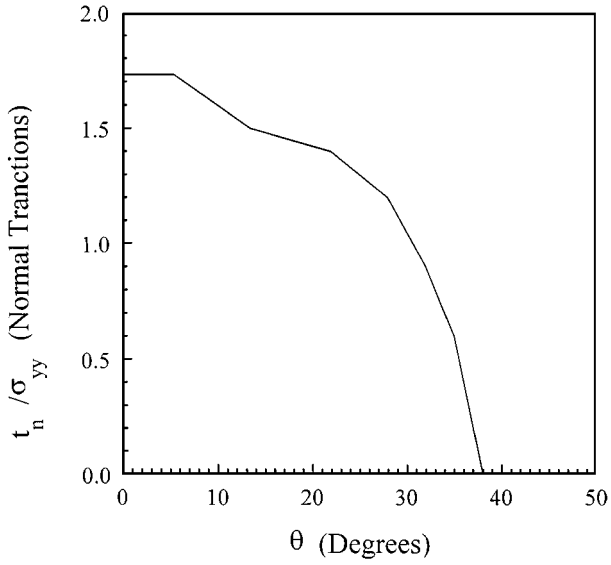

Figure 2 A plot of the normal interface tractions for a frictionally slipping interface of a composite ($\phi = 60^\circ$). The increase in the tractions at the top of the fiber is apparent [6].

The SiC_f/CAS composites ($\phi = 90^\circ$) were sliced in two directions. Fig. 3 shows the schematics of the preparation of the thin folis with $\theta = 0$ (a) and 90° (b) for the transmission electron microscopic (TEM) analyses. The composite slices (~ 1 mm thick) were glued on a glass slide with wax and polished down to 25 μm thickness by using mechanical polishing. Each thin foil specimen was mounted on a copper washer and brought to an ion milling machine for final thinning. Each specimen was analyzed for a microstructure and diffraction pattern by using Jeol 200CX transmission electron microscope (TEM) at 200 kV. Only the interfacial regions with a fiber diameter of about 15 μm were investigated both for the 0 and 90° samples since only the matrices adjacent to the fiber regions of about 15 μm width should be located at almost 0 and 90° around the fibers.

3. Results and discussion

Microstructures of the anorthite matrix in the composites deformed at a high temperature were analyzed and compared for the $\theta \sim 0$ and 90° samples. Fig. 4a shows the bright field image of the interfacial region of the composite ($\phi \sim 90^\circ$ and $\theta \sim 0^\circ$) deformed at 1290 °C (M: matrix, G: graphite, S: SiO_2 and F: SiC fiber). The SiO_2 and graphite layers are the products of oxidation of SiC fiber during composite fabrication (hot pressing). The CAS matrix shows a deformed structure with apparent dislocations, which indicates that the matrix near the $\theta \sim 0^\circ$ region was deformed by dislocation glide during the high-temperature creep deformation. In other words, the matrix above the top of the fiber ($\theta \sim 0^\circ$ area) was at a high stress level during the creep tests. Fig. 4b shows the selected area diffraction (SAD) pattern of the CAS matrix representing a triclinic structure. Also, a heavily twinned structure was observed for the $\theta \sim 0^\circ$ samples. Fig. 5 shows the twinned structure of of the CAS matrix (a) and SAD pattern from the twinned triclinic structure (b). The SAD pattern from the twinned triclinic structure was readily identified by the series of the three parallel spots.

Fig. 6a shows the bright field image of interfacial area of the composite ($\phi \sim 90^\circ$ and $\theta \sim 90^\circ$) deformed at 1290 °C. The matrix showed only the distinct twinned structure which implies that the $\theta \sim 90^\circ$ area was less stressed during the compressive creep deformation. Dislocations of extremely low density were observed in the matrix. The SAD pattern of the matrix in Fig. 6b indicates a twinned triclinic structure which also could be identified by the series of three parallel spots.

According to Meyer *et al.* [6] the anorthite matrix within the SiC_f/CAS composites deformed at the stress level of 35 MPa showed a stress exponent of near 3, indicating dislocation glide and/or mechanical twinning deformation. This is contrast to the result of $n \sim 2$ at 35 MPa for the deformation of pure anorthite matrix. They used a nonlinear Maxwell fluid constitutive model for the stress exponent of the composite. Their results revealed that the matrix in the composite has a stress exponent of ~ 1 for low stress level (< 15 MPa), and an increasing stress exponent for increasing compressive stress (~ 3 at 50 MPa). Since the matrix region right above the fiber of the composite was stressed significantly above the far-field stress ($t_n/\sigma_{yy} \sim 1.7; t_n > 50$ MPa) the stress exponent would increase from 2 to 3. Thus, it can be concluded that the region right above the fiber controls the high-temperature deformation of the composite. Due to the triclinic structure the dislocation glide in the anorthite matrix seems difficult since a triclinic crystal has the large, intrinsic Peierls stresses associated with the large Burgers vectors and does not include any obvious low-energy stacking faults for dissociation of dislocations into partials. However, since the stress level at the top of the fiber is very high the matrix would show the deformation associated with twinning and dislocation glide as well. The matrix remote from the top of the fiber ($\theta \sim 90^\circ$) which is at the relatively low stress level (35 MPa) showed a twinned structure and almost negligible density of dislocations. This result is in good agreement with that the pure matrix has the stress exponent of ~ 2 which indicates a partial diffusion creep and a partial mechanical twinning deformation.

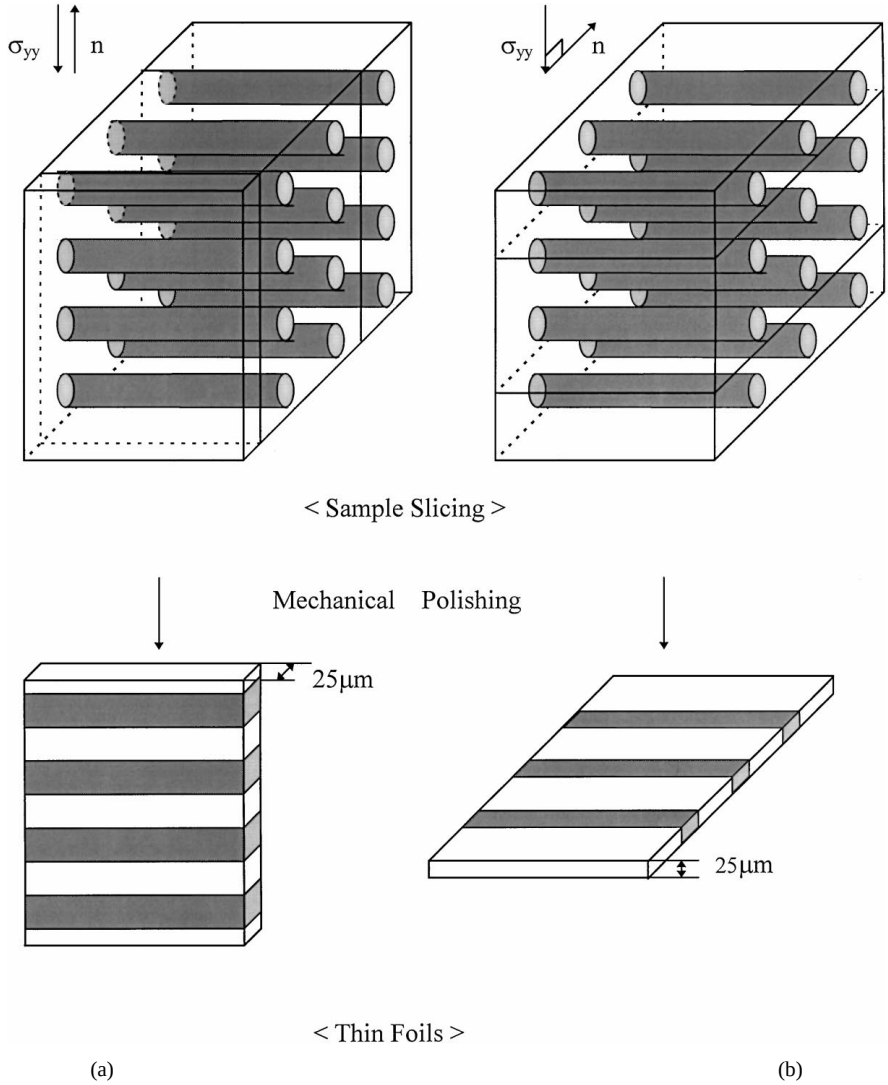

Figure 3 Schematics of TEM sample preparation out of SiC_f/CAS composites ($\phi \sim 90^\circ$); (a) $\theta \sim 0^\circ$ and (b) $\theta \sim 90^\circ$.

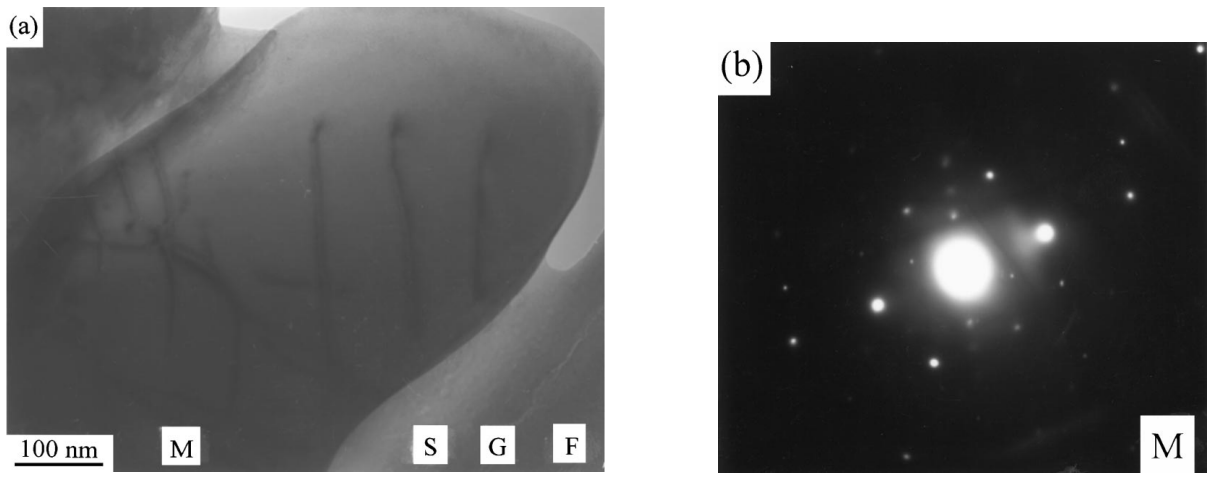

Figure 4 (a) A bright-field transmission electron micrograph (TEM) of the interfacial region of the silicon carbide fiber reinforced calcium aluminosilicate (CAS) glass-ceramic composite ($\phi \sim 90^\circ$ and $\theta \sim 0^\circ$) deformed at a high temperature. The CAS matrix shows the deformed structure by dislocation glide. (b) A corresponding selected area diffraction (SAD) pattern of the CAS matrix representing a triclinic structure.

4. Conclusions

The CAS matrix in the SiC_f/CAS composites deformed at 1290 °C showed high density of dislocations and twins at the region on the top of the SiC fiber ($\theta \sim 0^\circ$) and only twinned structure at the region remote from the top of the fiber ($\theta \sim 90^\circ$). The CAS matrix region on the top of the fiber must have been highly stressed compared to the region remote from the top of fiber since very high level of stress is required for the slip deformation in a triclinic crystal. This result agrees very well with the Meyer *et al.*'s mechanical modeling which predicted that in the SiC_f/CAS composite the traction

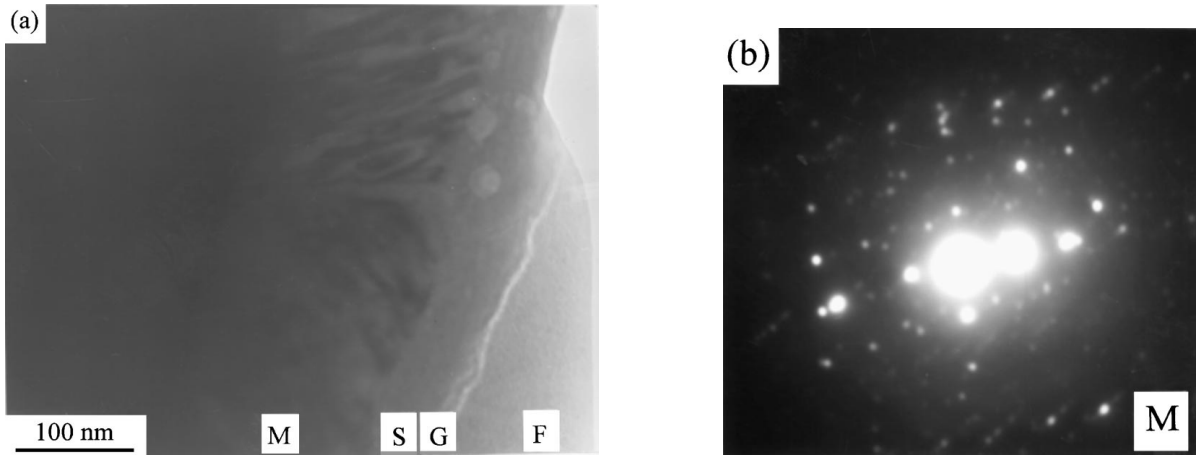

Figure 5 (a) A bright-field transmission electron micrograph (TEM) of the interfacial region of the silicon carbide fiber reinforced calcium aluminosilicate (CAS) glass-ceramic composite ($\phi \sim 90^\circ$ and $\theta \sim 0^\circ$) deformed at a high temperature. The CAS matrix shows the deformed structure by twinning. (b) A corresponding selected area diffraction (SAD) pattern of the CAS matrix representing a twinned clinic structure.

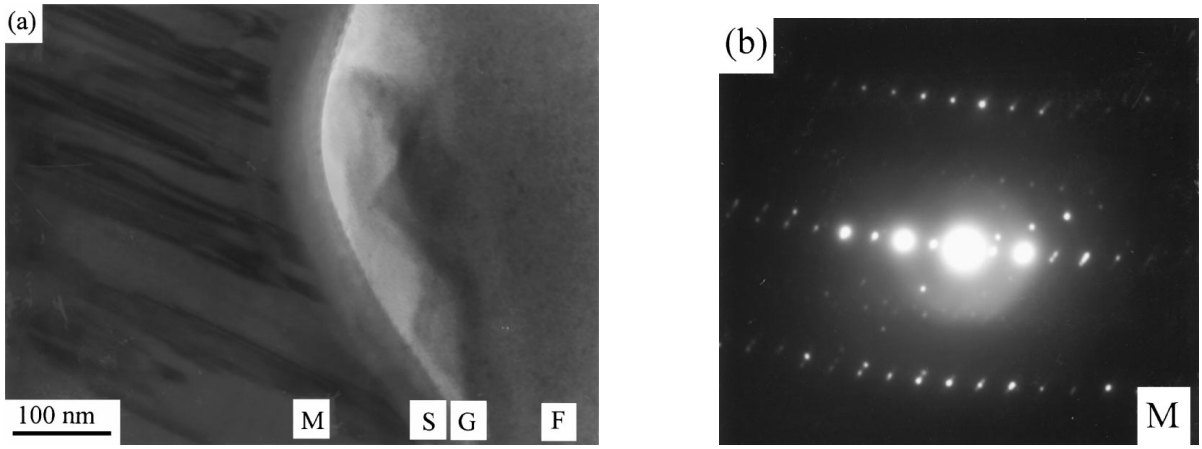

Figure 6 (a) A bright-field transmission electron micrograph (TEM) of the interfacial region of the silicon carbide fiber reinforced calcium aluminosilicate (CAS) glass-ceramic composite ($\phi \sim 90^\circ$ and $\theta \sim 90^\circ$) deformed at a high temperature. The CAS matrix shows an apparent twinned structure. (b) A corresponding selected area diffraction (SAD) pattern of the CAS matrix representing a twinned triclinic structure.

at the matrix above the top of the fiber is much higher than the remote stress.

Acknowledgements

The authors would like to thank Dr. Dallas W. Meyer at IBM, Rochester, Minnesota and Professor Reid F. Cooper at the University of Wisconsin-Madison for providing the opportunity to study the microstructure of SiC_f/CAS composites deformed at a high temperature. This work was partially supported by the Daejin University Research Grants of 1997.

References

1. R. F. COOPER and K. CHUNG, *J. Mater. Sci.* **22** (1987) 3148.
2. L. A. BONNEY and R. F. COOPER, *J. Amer. Ceram. Soc.* **73** (1990) 2916.
3. J. HOMENY, J. R. VANVALZAH and M. A. KELLY, *ibid.* **73** (1990) 2054.
4. F. ZOK, O. SBAIZERO, C. L. HOM and A. G. EVANS, *ibid.* **74** (1991) 187.
5. E. Y. SUN, S. R. NUTT and J. J. BRENNAN, *ibid.* **77** (1994) 1329.
6. F. ABBE, R. CARIN and J.-L. CHERMANT, *J. Eur. Ceram. Soc.* **5** (1989) 201.
7. A. H. CHOKSHI and J. R. PORTER, *J. Amer. Ceram. Soc.* **68** (1985) C-144.
8. F. ABBE, J. VICENS and J. L. CHERMANT, *J. Mater. Sci. Lett.* **8** (1989) 1026.
9. D. M. MEYER, R. F. COOPER and M. E. PLESHA, *Acta Metall. et Mater.* **41** (1993) 3157.
10. J. TULLIS, in "Feldspar Mineralogy," Vol. 2, edited by P. H. Ribbe (Mineralogical Society of America, 1983) p. 297.
11. D. B. MARSHALL and A. C. MCLAREN, *Phys. Chem. Min.* **1** (1977) 351.

Received 9 June 1997
and accepted 14 September 1998